ELSEVIER

International Journal of Heat and Fluid Flow 19 (1998) 556–562

International Journal of HEAT AND FLUID FLOW

Measurements and heat-flux transport modelling in a heated cylinder wake

Petra M. Wikström, Magnus Hallbäck, Arne V. Johansson *

Department of Mechanics, KTH, SE-100 44, Stockholm, Sweden

Abstract

Hot-wire measurements of velocity and temperature fluctuations have been made in the self-preserving turbulent wake region of a heated cylinder. Second order statistics including Reynolds fluxes, $\overline{u_i\theta}$, are determined along with relevant triple correlations appearing in the Reynolds stress and Reynolds flux transport equations. The primary aim with these measurements is to study different modelling levels for passive scalar quantities. Models for the pressure scalar-gradient correlation, appearing in the transport equation of the Reynolds fluxes, are compared to measured data. A significant improvement of the simplest model, $-c_{1T}(1/\tau)\overline{u_i\theta}$, is achieved by including a model for the rapid term that is linear in the mean velocity gradients. The mixed timescale, $\sqrt{k\overline{\theta^2}/\varepsilon\varepsilon_\theta}$, seems to be an appropriate choice for τ. Also models for the triple correlations, $\overline{u_iu_j\theta}$, are compared with the experiments.

1. Introduction

Turbulent transport of passive scalars plays an important part in many engineering applications and atmospheric flows. The passive scalar may for example be temperature, humidity, pollutant or any other chemical species. The transport equation of the mean scalar is given by

$$\frac{\partial\Theta}{\partial t}+U_l\frac{\partial\Theta}{\partial x_l}=\frac{\partial}{\partial x_l}\left(\alpha\frac{\partial\Theta}{\partial x_l}-\overline{u_l\theta}\right). \tag{1}$$

Here an unknown flux term, $\overline{u_i\theta}$, appears. In analogy with the eddy-viscosity concept this may be obtained by a simple gradient diffusion model,

$$\overline{u_i\theta}=-\frac{\nu_t}{\mathrm{Pr_t}}\frac{\partial\Theta}{\partial x_i}. \tag{2}$$

In a zero equation model an assumption of a constant turbulent Prandtl or Schmidt number is made. For many engineering applications this is not enough accurate. If the turbulent Prandtl or Schmidt number is not assumed to be constant, the transport equation of the scalar variance, $\overline{\theta^2}$, and the scalar dissipation rate, ε_θ, are needed to be solved for, in analogy with k–ε modelling. The simple eddy-diffusivity approach is unable to give a correct prediction of all components of $\overline{u_i\theta}$ in many flows. In the two-dimensional heated cylinder wake, for example, a zero prediction of the streamwise heat flux is obtained, whereas inclusion of a nonlinear term improves the situation considerably (Wikström et al., 1996). To involve more of the physics of heat flux transport, in the two-equation model approach, algebraic scalar-flux models which are obtained from the transport equations of the scalar fluxes may be used. The formulation of these involves the use of some equilibrium assumption equivalent to that used in algebraic Reynolds stress models. The basic platform here consists of transport equations of θ^2 and ε_θ. Explicit forms of these algebraic models are attractive since they lead to decreased numerical problems and computational efforts as compared to full second-order modelling. A second-order Reynolds flux model gives, in conjunction with a second-order Reynolds stress model, a turbulence closure consisting of twelve transport equations if the flow is three-dimensional.

The transport equation for the scalar fluxes, $\overline{u_i\theta}$, is given by

$$\frac{\partial\overline{u_i\theta}}{\partial t}+U_l\frac{\partial\overline{u_i\theta}}{\partial x_l}=-\overline{u_iu_l}\frac{\partial\Theta}{\partial x_l}-\overline{u_l\theta}\frac{\partial U_i}{\partial x_l}-\frac{\partial}{\partial x_l}\left(\overline{u_iu_l\theta}-\alpha\overline{\frac{\partial\theta}{\partial x_l}u_i}-\nu\theta\overline{\frac{\partial u_i}{\partial x_l}}\right)+\Psi_i, \tag{3}$$

$$\Psi_i=-\frac{\partial}{\partial x_l}\left(\overline{\frac{p}{\rho}\theta\delta_{il}}\right)+\overline{\frac{p}{\rho}\frac{\partial\theta}{\partial x_i}}-(\alpha+\nu)\overline{\frac{\partial\theta}{\partial x_l}\frac{\partial u_i}{\partial x_l}}. \tag{4}$$

The right-hand side of the transport equation contains two production terms, a transport term consisting of one turbulent and two molecular diffusion terms, a pressure-transport term, a pressure scalar-gradient correlation term and diffusive and viscous destruction. The sum of these three last terms is here denoted by Ψ_i. At high Reynolds numbers the molecular diffusion terms are small compared to the turbulent ones and may be neglected. Also the viscous and diffusive destruction terms should then be negligible, since the small scales are nearly isotropic at high Reynolds numbers. By modelling the turbulent diffusion, $-(\partial/\partial x_l)(\overline{u_iu_l\theta})$, and Ψ_i a modelled differential Reynolds-flux equation is obtained. Through approximation of the modelled transport equation we may obtain an algebraic scalar-flux model, in which the model for Ψ_i would be one of the ingredients.

* Corresponding author. E-mail: johansson@mech.kth.se.

0142-727X/98/$ – see front matter
PII: S0142-727X(98)10018-8

When modelling the transport equation for the turbulent scalar fluxes, a model for the pressure scalar-gradient correlation term is needed. This term may be divided into a slow part and a rapid part, where the slow part modelled by $-c_{1T}(1/\tau)\overline{u_i\theta}$, may also include effects of destruction (Shih, 1996). Two major questions now arise. What is the appropriate timescale, τ, and when are the rapid terms important? Launder (1978) suggested that both the thermal and the dynamical timescales are important. Since they are generally not proportional, i.e. Pr_t is not constant, a mixture of these should then be used to blend both thermal and mechanical contributions. An objection to this approach could be that inclusion of the thermal timescale results in a violation of the superposition principle for passive scalars. On the other hand, the analog violation is made in nonlinear models of the pressure–strain rate. In a DNS of homogeneous shear flow by Rogers et al. (1989), it was found that the sum of the pressure scalar-gradient and the destruction terms, in the turbulent scalar flux transport equation, are approximately aligned with the flux vector itself. However, such an alignment does not exclude the possibility to substantially improve the predictions by including rapid terms when modelling these terms. Effects of the rapid terms in the flow field downstream a heated cylinder are investigated in the present paper.

2. Experimental procedure

The MTL wind tunnel, at KTH, Stockholm, with a 7.0 m long test section of 1.2×0.8 m^2 cross-section and a free stream turbulence level less than 0.05% was used in the experiments. The diameter of the wake-generating cylinder was 6.4 mm and all the measurements were made at a velocity, U_0, of 10.1 m/s giving a maximum mean velocity deficit of 0.5 m/s at $x/d = 400$. The present Reynolds number, $U_0 d/\nu = 4300$, is about three times higher than that of Browne and Antonia (1986). The cylinder was electrically heated giving a maximum mean temperature excess, Θ_s, of 0.8°C above the ambient air temperature at $x/d = 400$. Measurements were made at the following four different downstream positions: $x/d = 200$, 400, 600 and 800. The streamwise variations of the maximum velocity defect, U_s, the maximum temperature excess, Θ_s, and the velocity defect half-width, l, are in good agreement with those of Browne and Antonia (Wikström et al., 1996). The results presented below are obtained from data at $x/d = 400$, where the turbulent Reynolds number, $4k^2/\nu\varepsilon$, is about 3200 at the location of maximum production. Here k is the turbulent kinetic energy and ε is the dissipation rate of k.

Simultaneous measurements of velocity and temperature statistics were made using a three-wire probe configuration consisting of an X-probe for velocity measurements and a single cold wire for temperature detection, located 0.5 mm in front of the X-wire mid point. The hot wires had a length of 0.5 mm and a diameter of 2.5 μm. The corresponding dimensions for the cold wire were 1.0 mm and 0.63 μm. Voltages from the constant temperature and constant current circuits were filtered at 5 kHz and sampled at 10 kHz.

Cross-stream derivatives of measured quantities were obtained by using cubic-spline smoothing. Derivatives in the streamwise direction, needed to determine advective terms, were obtained by assuming self-similarity. It was demonstrated that this assumption was valid at $x/d = 400$.

3. Results

In Figs. 1 and 2 the dominating terms in the transport equations for $\overline{u\theta}$ and $\overline{v\theta}$ are shown. Molecular diffusion as well as terms involving streamwise derivatives may be neglected. All terms are measured except Ψ_i which is obtained by balancing Eq. (3). The two components of Ψ_i are then given by

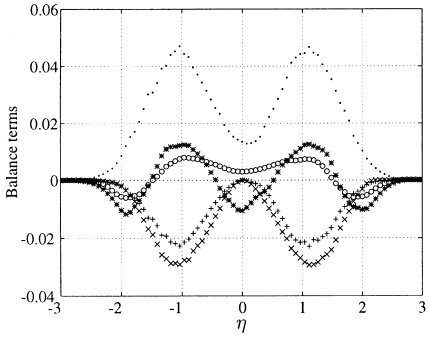

Fig. 1. The dominating terms in the transport equation of $\overline{u\theta}$ normalized by $U_s^2\Theta_s/l$, where l is the velocity defect half-width and $\eta = y/l$. ∘, $U\partial\overline{u\theta}/\partial x$; +, $-\overline{uv}\partial\Theta/\partial y$; ×, $-\overline{v\theta}\partial U/\partial y$; ∗, $-(\partial/\partial y)\overline{uv\theta}$; ·, Ψ_1.

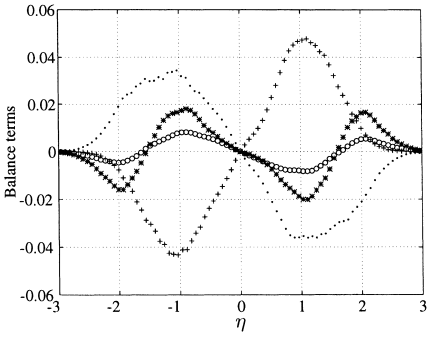

Fig. 2. The dominating terms in the transport equation of $\overline{v\theta}$ normalized by $U_s^2\Theta_s/l$, where l is the velocity defect half-width and $\eta = y/l$. ∘, $U\partial\overline{v\theta}/\partial x$; +, $-\overline{v^2}\partial\Theta/\partial y$; ∗, $-(\partial/\partial y)\overline{v^2\theta}$; ·, Ψ_2.

$$\Psi_1 = U\frac{\partial\overline{u\theta}}{\partial x} + \overline{uv}\frac{\partial\Theta}{\partial y} + \overline{v\theta}\frac{\partial U}{\partial y} + \frac{\partial}{\partial y}\overline{uv\theta}, \tag{5}$$

$$\Psi_2 = U\frac{\partial\overline{v\theta}}{\partial x} + \overline{v^2}\frac{\partial\Theta}{\partial y} + \frac{\partial}{\partial y}\overline{v^2\theta}. \tag{6}$$

Here, these are of the same order as the rest of the terms and may not be neglected. In the case of Ψ_1, though, the inhomogeneous term, $-(\partial/\partial x)\overline{(p/\rho)\theta}$, may be neglected in the present flow situation. Measurements of $(\partial\theta/\partial t)$ $(\partial u_i/\partial t)$ indicate that about 3% of Ψ_1 and 15% of Ψ_2 are contributions from the destruction terms in the present experiment. Figs. 1 and 2 also show that the turbulent diffusion terms are significant and may not be neglected.

3.1. Model comparison for Ψ_i

In Fig. 3 the inclination angles of the turbulent scalar flux, $\overline{u_i\theta}$, and Ψ_i are compared. In this figure we see that Ψ_i is approximately parallel to the heat-flux vector and oriented in the opposite direction. This result is similar to what has been found by Rogers et al. (1989). A linear relaxation relation, $\Psi_i = -c_{1T}(1/\tau)\overline{u_i\theta}$, seems from this figure to be a good candidate for modelling Ψ_i, where τ often is taken as the dynamical timescale, k/ε.

The following, more general, model for Ψ_i will be compared with the present data:

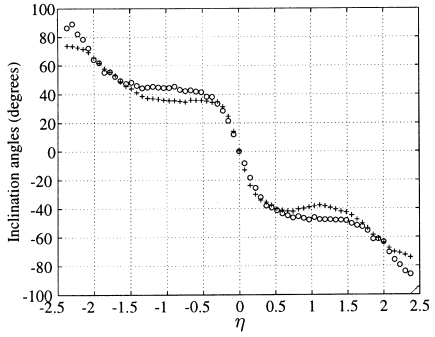

Fig. 3. Comparison between the inclination angles of the turbulent scalar flux, $\overline{u_i\theta}$, and Ψ_i. ∘, $\tan^{-1}(\overline{v\theta}/\overline{u\theta})$; +, $\tan^{-1}(\Psi_2/\Psi_1)$.

$$\Psi_i = -c_{1T}\frac{1}{\tau}\overline{u_i\theta} + c_{2T}\overline{u_l\theta}U_{i,l} + c_{3T}\overline{u_l\theta}U_{l,i}. \tag{7}$$

This form is obtained by neglecting the destruction and the pressure-diffusion terms in Eq. (4), and modelling the slow part of the pressure scalar-gradient term by the first term on the right-hand side of Eq. (7), and the rapid part by the second and third terms. The slow part may also include effects of destruction. In the present plane shear flow the c_{2T} term contributes only to the Ψ_1 component and the c_{3T} term contributes only to the Ψ_2 component.

The DNS of homogeneous shear flow by Rogers et al. gives a constant timescale ratio, $\overline{\theta^2}\varepsilon/k\varepsilon_\theta$, of about 1.2, where ε_θ is the dissipation rate of $\frac{1}{2}\overline{\theta^2}$. An estimation of ε has been made from the present data by balancing the transport equation of k and neglecting the pressure-diffusion term. The timescale ratio, based on this estimate, ranges from about 0.9 at the centerline to 0.6 at the point of maximum production, which may be seen in Fig. 4. The estimated timescale ratio is thus not constant in the present wake flow. The timescale ratio in some cases including the heated cylinder is discussed by Béguier and Dekeyser (1978) and Launder (1978). In the comparisons below three different timescales will be used for τ: the dynamical timescale, k/ε, the thermal timescale, $\overline{\theta^2}/\varepsilon_\theta$, where ε_θ was determined from the $\overline{\theta^2}$-equation, and a mixed timescale, $\sqrt{k\overline{\theta^2}}/\varepsilon\varepsilon_\theta$, which blends both thermal and mechanical contributions.

In Figs. 5–10 Ψ_1 and Ψ_2 obtained from the measured data are compared with those obtained from Eq. (7) using the values of c_{1T}, c_{2T} and c_{3T} given in Table 1 and the three different choices of the timescale. c_{1T} is the same, 3.2, for all models, whereas c_{2T} and c_{3T} are varied. In model (a) c_{2T} and c_{3T} are set to zero and Eq. (7) then gives a model of Ψ_i aligned with the heat-flux vector. The parameter choice of model (b) is $c_{1T} = 3.2$, $c_{2T} = 0.50$ and $c_{3T} = 0$. If the timescale is taken to be the dynamical timescale, k/ε, we have the Launder (1975) model. By formal solution of the Poisson equation for the rapid pressure a linear model for $\overline{(p/\rho)(\partial\theta/\partial x_i)}$ may be derived, see e.g. Shih (1996). Mathematical constraints then give $c_{2T} = \frac{4}{5}$ and $c_{3T} = -\frac{1}{5}$. These parameter choices are used in model (c).

In Figs. 5 and 6 the timescale τ is taken to be k/ε as in the Launder model. All models give a very good agreement at the centerline, which simply reflects that an appropriate value of c_{1T} has been chosen. Model (a) underpredicts both the Ψ_1

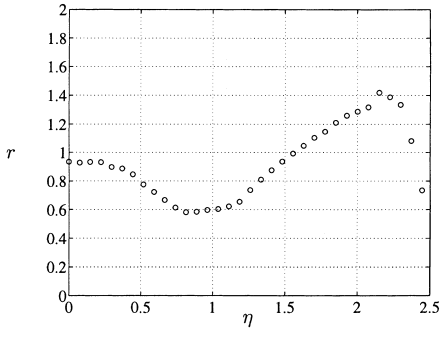

Fig. 4. The time-scale ratio $r = \overline{\theta^2}\varepsilon/k\varepsilon_\theta$.

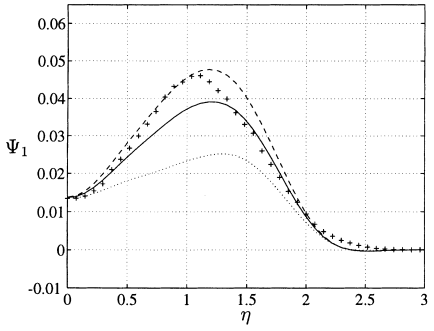

Fig. 5. Comparison between Ψ_1 (normalized by $U_s^2\Theta_s/l$) obtained from the experimental data and that obtained from Eq. (7) using the parameter values of c_{1T}, c_{2T} and c_{3T} given in Table 1. +, experimental data; ···, (a); ——, (b); - - -, (c), with $\tau = k/\varepsilon$.

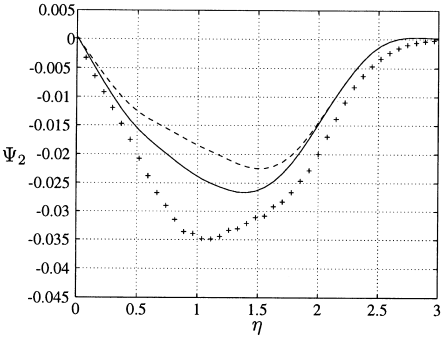

Fig. 6. Comparison between Ψ_2 (normalized by $U_s^2\Theta_s/l$) obtained from the experimental data and that obtained from Eq. (7) using the parameter values of c_{1T}, c_{2T} and c_{3T} given in Table 1. +, experimental data; ——, (a) and (b); - - -, (c), with $\tau = k/\varepsilon$.

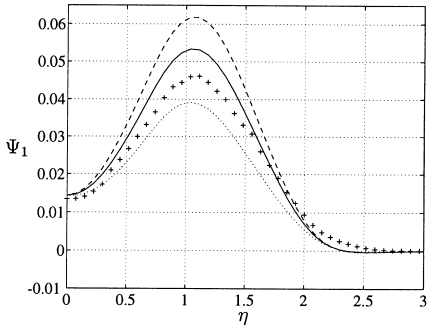

Fig. 7. Comparison between Ψ_1 (normalized by $U_s^2\Theta_s/l$) obtained from the experimental data and that obtained from Eq. (7) using the parameter values of c_{1T}, c_{2T} and c_{3T} given in Table 1. +, experimental data; ···, (a); ——, (b); - - -, (c), with $\tau = \overline{\theta^2}/\varepsilon_\theta$.

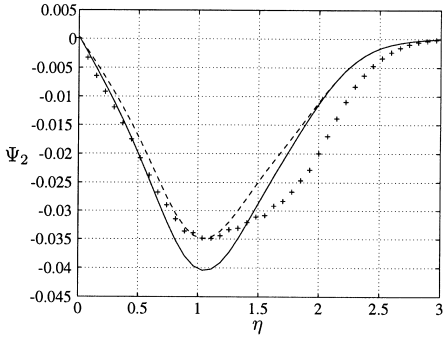

Fig. 8. Comparison between Ψ_2 (normalized by $U_s^2\Theta_s/l$) obtained from the experimental data and that obtained from Eq. (7) using the parameter values of c_{1T}, c_{2T} and c_{3T} given in Table 1. ——, (a) and (b); - - -, (c), with $\tau = \overline{\theta^2}/\varepsilon_\theta$.

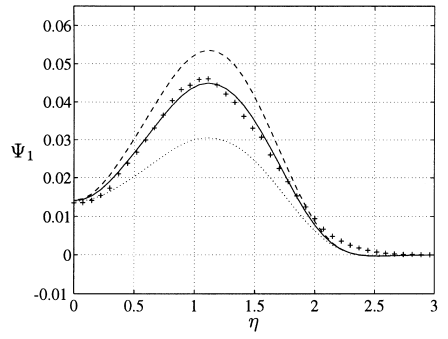

Fig. 9. Comparison between Ψ_1 (normalized by $U_s^2\Theta_s/l$) obtained from the experimental data and that obtained from Eq. (7) using the parameter values of c_{1T}, c_{2T} and c_{3T} given in Table 1. +, experimental data; $\cdots$, (a); ——, (b); - - -, (c), with $\tau = \sqrt{k\overline{\theta^2}/\varepsilon\varepsilon_\theta}$.

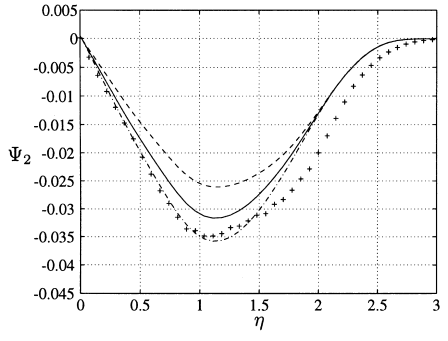

Fig. 10. Comparison between Ψ_2 (normalized by $U_s^2\Theta_s/l$) obtained from the experimental data and that obtained from Eq. (7) using the parameter values of c_{1T}, c_{2T} and c_{3T} given in Table 1. +, experimental data; ——, (a) and (b); - - -, (c); – · –, $c_{1T} = 3.2$, $c_{2T} = 0.50$ and $c_{3T} = 0.15$, with $\tau = \sqrt{k\overline{\theta^2}/\varepsilon\varepsilon_\theta}$.

Table 1
The different combinations of the model constants used in Eq. (7) (models (a) and (b) are equivalent for the Ψ_2-component)

Model	c_{1T}	c_{2T}	c_{3T}
(a)	3.2	0	0
(b)	3.2	0.50	0
(c)	3.2	$\frac{4}{5}$	$-\frac{1}{5}$

and Ψ_2 components. The Launder model, (b), gives the same prediction as the previous one in the case of the Ψ_2 component, but improves the prediction of the Ψ_1 component. Hence, inclusion of the rapid term gives an improvement. Model (c) is unable to predict the two components simultaneously and gives a severe underprediction of the Ψ_2 term. The Launder model could give a better compromise for the components by increasing c_{1T} to 4.0, though, resulting in a overprediction of about 20% of the Ψ_1 component at the centerline.

For the models in Figs. 5 and 6 the prediction of the peak is displaced towards the freestream compared to the measured data. This could be due to the neglection of the pressure-diffusion term when determining ε needed in the dynamical timescale, k/ε. A comparison has been made with the model predictions obtained when using the directly measured ε of Aronson and Löfdahl (1994) in the timescale, k/ε. In this case the displacement of the peaks is not obtained, whereas the maximum amplitudes will be the same as with the estimate of ε from the present data.

In Figs. 7 and 8 the timescale τ is taken to be the thermal timescale, $\overline{\theta^2}/\varepsilon_\theta$. Since the timescale ratio is 0.9 at the centerline all models give good agreement here as in the previous case. Model (c) gives a good prediction of the maximum amplitude of the Ψ_2 component, whereas the Ψ_1 component is overpredicted. Model (b) gives an overprediction of both components. The larger values at $\eta = 1$, compared to the previous case, of all model predictions are due to that the timescale ratio is 0.6 at this position. By using $c_{1T} = 2.8$ instead of 3.2 in model (b) the behavior of both components is well captured.

In Figs. 9 and 10 the timescale τ is taken to be the mixed timescale $\sqrt{k\overline{\theta^2}/\varepsilon\varepsilon_\theta}$. As in the previous cases models (a) and (c) are unable to predict the two components simultaneously and all models give good agreement at the centerline. Model (b) gives a very good prediction of the Ψ_1 component, whereas Ψ_2 is slightly underpredicted. This could be due to the fact that Ψ_2 contains also a pressure-diffusion term and the experimental data of this component seems to be more contaminated by the destruction term. Using $c_{1T} = 3.5$ instead of 3.2 in model (b), a better compromise for the two components is obtained, while by choosing c_{3T} in model (b) to be 0.15 instead of 0, the prediction of Ψ_2 can be improved while the prediction of Ψ_1 is unchanged.

3.1.1. Comparison with an extended model

The inclusion of a fourth term, involving mean temperature gradients, in the model for Ψ_i has been used by previous workers (see Shabany and Durbin, 1997):

$$\Psi_i = -c_{1T}\frac{1}{\tau}\overline{u_i\theta} + c_{2T}\overline{u_l\theta}U_{i,l} + c_{3T}\overline{u_l\theta}U_{l,i} + c_{4T}\overline{u_iu_l}\Theta_{,l}. \tag{8}$$

Figs. 11 and 12 show the prediction of Eq. (8) using the parameter values given in Table 2. In model (b) the fourth term is excluded, that is $c_{4T} = 0$, and in model (c) the parameter choice $c_{2T} = 1$ and $c_{3T} = 0$ is made. All the other parameters are obtained by a least-square fit to the two components of Ψ_i simultaneously, using the mixed timescale, $\sqrt{k\overline{\theta^2}/\varepsilon\varepsilon_\theta}$. Model (a) gives a very good agreement, whereas model (b) is almost as good except for a slight overprediction near the centerline in the case of the Ψ_1-component. The signs of the c_{2T} and c_{3T} parameters in model (b) are the same as in the theoretical derivation.

In a new explicit algebraic scalar-flux model by Wikström et al. (1997), the parameter choice $c_{2T} = 1$ and $c_{3T} = 0$ gives a significant simplification of the model formulation. The model prediction (c) shows that a fairly reasonable agreement

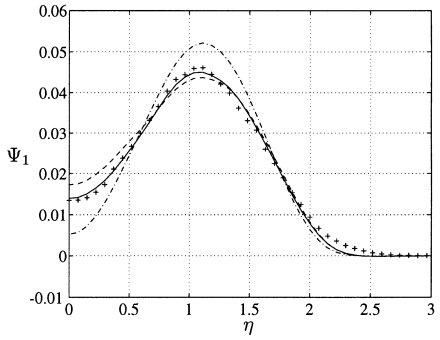

Fig. 11. Comparison between Ψ_1 (normalized by $U_s^2\Theta_s/l$) obtained from the experimental data and that obtained from Eq. (8) using the parameter values of c_{1T}, c_{2T}, c_{3T} and c_{4T} given in Table 2. +, experimental data; ——, (a); - - -, (b); – · –, (c), with $\tau = \sqrt{k/\overline{\theta^2}}/\varepsilon\varepsilon_\theta$.

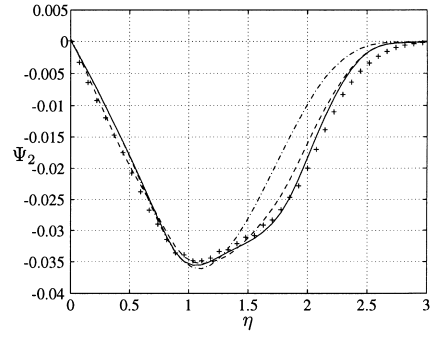

Fig. 12. Comparison between Ψ_2 (normalized by $U_s^2\Theta_s/l$) obtained from the experimental data and that obtained from Eq. (8) using the parameter values of c_{1T}, c_{2T}, c_{3T} and c_{4T} given in Table 2. +, experimental data; ——, (a); - - -, (b); – · –, (c), with $\tau = \sqrt{k/\overline{\theta^2}}/\varepsilon\varepsilon_\theta$.

may be obtained with this parameter choice in the present flow case.

3.2. Model comparison for $\overline{u_iu_j\theta}$

The following model for the triple correlations, $\overline{u_iu_j\theta}$, is here compared to the experimental data:

$$\begin{aligned}\overline{u_iu_j\theta} = {} & \alpha_1 k\tau\left(\overline{u_l\theta}\right)_{,l}\delta_{ij} + \alpha_2 k\tau\left[\left(\overline{u_i\theta}\right)_{,j} + \left(\overline{u_j\theta}\right)_{,i}\right] \\ & + \tau\Big\{\alpha_3\left[\overline{u_iu_l}\left(\overline{u_j\theta}\right)_{,l} + \overline{u_ju_l}\left(\overline{u_i\theta}\right)_{,l}\right] + \alpha_4\overline{u_iu_j}\left(\overline{u_l\theta}\right)_{,l} \\ & + \alpha_5\left[\overline{u_iu_l}\left(\overline{u_l\theta}\right)_{,j} + \overline{u_ju_l}\left(\overline{u_l\theta}\right)_{,i}\right] + \alpha_6\overline{u_l\theta}\left(\overline{u_iu_j}\right)_{,l} \\ & + \alpha_7\left[\overline{u_i\theta}\left(\overline{u_ju_l}\right)_{,l} + \overline{u_j\theta}\left(\overline{u_iu_l}\right)_{,l}\right] + \alpha_8\left[\overline{u_l\theta}\left(\overline{u_ju_l}\right)_{,i} \right. \\ & \left. + \overline{u_l\theta}\left(\overline{u_iu_l}\right)_{,j}\right] + \alpha_9\left[\overline{u_j\theta}\left(\overline{u_iu_l}\right)_{,i} + \overline{u_i\theta}\left(\overline{u_lu_l}\right)_{,j}\right]\Big\}. \end{aligned} \tag{9}$$

Table 2
The parameter values in Eq. (8) obtained from a least-square fit to the experimental data using all four terms, (a), and only the three first terms, (b), with $\tau = \sqrt{k/\overline{\theta^2}}/\varepsilon\varepsilon_\theta$

Model	c_{1T}	c_{2T}	c_{3T}	c_{4T}
(a)	3.2	−0.05	−1.0	0.70
(b)	4.0	0.18	−0.16	0
(c)	1.2	1	0	0.54

All the coefficients may be seen as functions of the invariants of the tensors in Eq. (9) but will here be considered as constants. If the timescale, τ, is taken as the dynamical timescale, the Shih (1996) model is obtained, where also higher order terms may be included. In a plane wake flow this model gives a zero prediction of the triple correlations $\overline{uw\theta}$ and $\overline{vw\theta}$, which is expected and in agreement with the experimental data. The other four nonzero components, $\overline{u^2\theta}$, $\overline{v^2\theta}$, $\overline{w^2\theta}$ and $\overline{uv\theta}$, are shown in Figs. 13–16. The derivatives $-(\partial/\partial y)\overline{v^2\theta}$ and $-(\partial/\partial y)\overline{uv\theta}$ appear as the diffusion terms in the transport equations of the heat fluxes, in the present flow case. Figs. 13–16 also show the prediction of Eq. (9) using the parameter values given in Table 3. The parameters of model (a) are obtained by a least-square fit to all four nonzero components simultaneously, using the mixed timescale, $\sqrt{k/\overline{\theta^2}}/\varepsilon\varepsilon_\theta$. This model predicts all components quite well, though, the behavior of $\overline{u^2\theta}$ and $\overline{w^2\theta}$ are somewhat mispredicted for $\eta < 1$. Model (b) is also a least-square fit to the experimental data, but here only the α_2 and α_6 terms are included. This model gives predictions quite close to those of model (a) for all four components considering that only two model parameters are used instead of nine. Using the α_3-term instead of the α_2-term, gives approximately the same predictions as that of model (b). The inclusion of a tensor eddy diffusivity thus makes no major difference in the present flow case. The α_3-term could of course be of

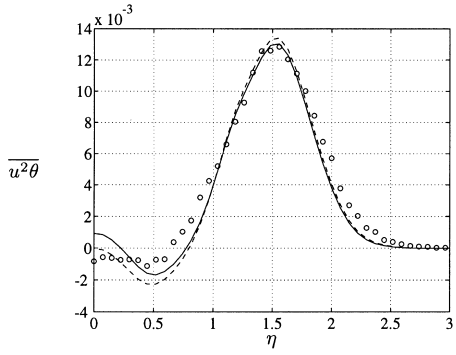

Fig. 13. Comparison between $\overline{u^2\theta}$ (normalized by $U_s^2\Theta_s$) obtained from the experimental data and that obtained from Eq. (9) using the parameter values given in Table 3. ○, experimental data; ——, (a); - - -, (b), with $\tau = \sqrt{k/\overline{\theta^2}}/\varepsilon\varepsilon_\theta$.

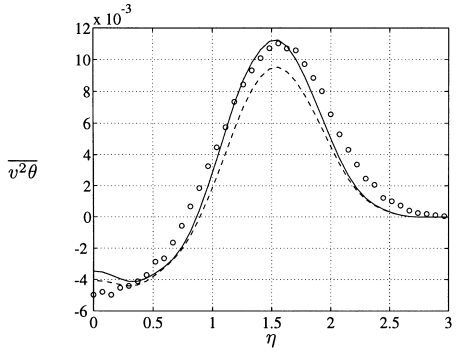

Fig. 14. Comparison between $\overline{v^2\theta}$ (normalized by $U_s^2\Theta_s$) obtained from the experimental data and that obtained from Eq. (9) using the parameter values given in Table 3. ○, experimental data; ——, (a); - - -, (b), with $\tau = \sqrt{k/\overline{\theta^2}}/\varepsilon\varepsilon_\theta$.

Table 3
The parameter values in Eq. (9) obtained from a least-square fit to the experimental data using all nine terms, (a), and only two terms, (b), with $\tau = \sqrt{k\overline{\theta^2}/\varepsilon\varepsilon_\theta}$

Model	α_1	α_2	α_3	α_4	α_5	α_6	α_7	α_8	α_9
(a)	0.017	−0.12	−0.064	0.028	0.093	−0.51	−0.0072	0.10	−0.062
(b)	0	−0.072	0	0	0	−0.54	0	0	0

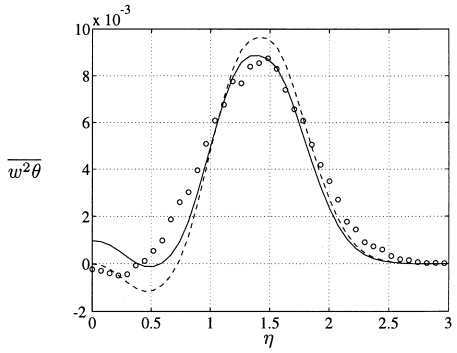

Fig. 15. Comparison between $\overline{w^2\theta}$ (normalized by $U_s^2\Theta_s$) obtained from the experimental data and that obtained from Eq. (9) using the parameter values given in Table 3. ○, experimental data; ——, (a); - - -, (b), with $\tau = \sqrt{k\overline{\theta^2}/\varepsilon\varepsilon_\theta}$.

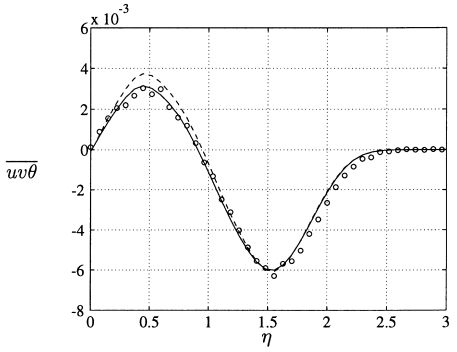

Fig. 16. Comparison between $\overline{uv\theta}$ (normalized by $U_s^2\Theta_s$) obtained from the experimental data and that obtained from Eq. (9) using the parameter values given in Table 3. ○, experimental data; ——, (a); - - -, (b), with $\tau = \sqrt{k\overline{\theta^2}/\varepsilon\varepsilon_\theta}$.

importance in a flow with a higher degree of anisotropy. In the present flow case the α_6-term seems to be of major importance. This term as well as the α_4-term are the only ones giving a nonzero prediction of the $\overline{w^2\theta}$ component in the present flow case. If the dynamical timescale is used instead of the mixed timescale when deriving the two least-square fits to the experimental data, approximately the same model predictions are obtained but with different values of the model parameters. For example the parameters of model (b) would then be $\alpha_2 = -0.064$ and $\alpha_6 = -0.43$.

4. Conclusions

From the present experimental data it seems clear that a significant improvement to the simplest model, $\Psi_i = -c_{1T}(1/\tau)\overline{u_i\theta}$, can be achieved by including a linear model for the rapid part of the pressure scalar-gradient term. By using a mixed timescale, $\sqrt{k\overline{\theta^2}/\varepsilon\varepsilon_\theta}$, the curves of the two components of Ψ_i are best captured. With this choice of the timescale the following parameter choice gives the most satisfactory model prediction for this flow situation: $c_{1T} = 3.2$, $c_{2T} = 0$, $c_{3T} = -1.0$ and $c_{4T} = 0.7$. In a DNS of scalar transport in homogeneous turbulence by Kawamura and Ihira (1996) it was found that c_{1T} depends on the turbulent Reynolds number and has a value of 3.8, using the dynamical timescale, for high Reynolds numbers. In the present case the Launder model gives a reasonably good compromise for both the components of Ψ_i by increasing c_{1T} from 3.2 to 4.0. From Eq. (7) it is evident that the rapid terms are important when the velocity gradients become of the same order of magnitude as the inverse of the timescale, τ, since the model constants all are of the same order of magnitude.

When using the truncated Shih model for the triple correlations, $\overline{u_iu_j\theta}$, given in Eq. (9), only two of the terms may give approximately as good predictions as those of a model including all nine terms. These two terms are the α_2-term and α_6-term, where the latter ensures a nonzero prediction of $\overline{w^2\theta}$ in the present flow case. A simple gradient diffusion model, though, given by the α_2-term, using a constant eddy-diffusivity, or the α_3-term, using a tensor eddy-diffusivity, are here unable to capture the behavior of this component. Inclusion of a tensor eddy-diffusivity, i.e., using the α_3 instead of the α_2-term together with the α_6-term, gives no improvement and thus seems to be of less importance in the present wake flow.

References

Aronson, D., Löfdahl, L., 1994. The plane wake of a cylinder: An estimate of the pressure-strain rate tensor. J. Fluid Mech. 67, 569–581.

Béguier, C., Dekeyser, I., 1978. Ratio of scalar and velocity dissipation time scales in shear flow turbulence. Phys. Fluids A 21, 307–310.

Browne, L.W.B., Antonia, R.A., 1986. Reynolds shear stress and heat flux measurements in a cylinder wake. Phys. Fluids A 29, 709–713.

Kawamura, H., Ihira, H., 1996. DNS and modeling of scalar transport in homogeneous turbulence. In: Rodi, Bergeles (Eds.), Engineering Turbulence Modelling and Experiments 3. Elsevier, Amsterdam, pp. 239–249.

Launder, B.E., 1975. On the effects of a gravitational field on the turbulent transport of heat and momentum. J. Fluid Mech. 67, 569–581.

Launder, B.E., 1978. Heat and mass transport. In: Bradshaw (Ed.), Topics in Physics, vol. 12. Springer, New York, pp. 231–287.

Rogers, M.M., Mansour, N.N., Reynolds, W.C., 1989. An algebraic model for the turbulent flux of a passive scalar. J. Fluid Mech. 203, 77–101.

Shabany, Y., Durbin, P.A., 1997. Explicit algebraic scalar flux approximation. AIAA J. 35, 985–989.

Shih, T.H., 1996. In: Hallbäck et al. (Eds.), Turbulence and transition modeling, Chap. 4. Kluwer ERCOFTAC Series.

Wikström, P.M., Hallbäck, M., Johansson, A.V., 1996. Measurements and modeling of temperature fluctuations in a heated cylinder wake. In: Chen et al. (Eds.), Flow Modeling and Turbulence Measurements VI, Balkema, pp. 143–150.

Wikström, P.M., Wallin, S., Johansson, A.V., 1997. Explicit algebraic modelling of passive scalar flux. Seventh ETC Conference 1998, submitted.